Advances in Nanoparticles, 2015, 4, 85-97
Published Online November 2015 in SciRes. http://www.scirp.org/journal/anp
http://dx.doi.org/10.4236/anp.2015.44010

Thermal Stability and Hot Carrier Dynamics of Gold Nanoparticles of Different Shapes

Yasser A. Attia[1,2,3], Tariq A. Altalhi[2], Adil A. Gobouri[2]

[1]National Institute of Laser Enhanced Sciences, Cairo University, Giza, Egypt
[2]Department of Chemistry, Faculty of Science, Taif University, Taif, Kingdom of Saudi Arabia
[3]Department of Physical Chemistry, Faculty of Chemistry, Santiago de Compostela University, Santiago de Compostela, Spain
Email: yasserniles@niles.edu.eg, tmmba@windowslive.com

Received 25 August 2015; accepted 6 November 2015; published 9 November 2015

Abstract

Anisotropic shapes of gold nanoparticles are prepared using a modified seed method in the presence of silver ions or clusters in order to study the thermal stability and the dynamics of the hot carriers induced by femtosecond laser pulses. Although gold nanospheres are stable towards thermal treatment, the decomposition of the gold nanorods into spherical nanoparticle aggregates upon thermal treatment is mechanistically different from the case of nanoprisms. Great enhancement of thermal stability is achieved by modifying the surface of the nanoparticles by adding specific amounts of polyvinyl pyrrolidone (PVP) after preparation of gold particles of different shapes capped with cetyltrimethylammonium bromide (CTAB). The surface plasmon resonance spectra of the gold nanostructures are used to monitor their morphological changes. In regards to the hot carrier dynamics, it is found that the phonon-phonon (ph-ph) coupling is much slower in dots than in rods and prisms while electron-phonon (e-ph) coupling is almost the same in these particles.

Keywords

Thermal Reshaping, Stability, Relaxation Dynamics, Anisotropic Gold Nanoparticles, Femtosecond Laser, Capping Materials

1. Introduction

One of the desired goals is to overcome the challenge of controlling the morphology of the nanoparticles, and to be able to fabricate and stabilize them in the desired form. The electrical, thermodynamic, and physicochemical properties of metal nanoparticles depend sensitively on particle size and shape [1] [2]. There are different me-

How to cite this paper: Attia, Y.A., Altalhi, T.A. and Gobouri, A.A. (2015) Thermal Stability and Hot Carrier Dynamics of Gold Nanoparticles of Different Shapes. *Advances in Nanoparticles*, **4**, 85-97. http://dx.doi.org/10.4236/anp.2015.44010

thods to prepare different shapes of gold nanoparticles but the most common one is the seed-mediated method which is developed by Murphy's group and further improved by El-Sayed's group [3]-[9].

Controlling the shape, morphology, and size can be useful in understanding of the electron dynamics and the relaxation processes in gold nanoparticles, which is required because of their fast optical response. This is very important for many potential applications such as optical switching, electronic devices, and biomedical sensing and diagnostics applications [8]-[14]. Moreover, better understanding of properties such as electrical and thermal conductivity and superconductivity of metal nanoparticles could be achieved by studying the relaxation dynamics.

In gold nanoparticles, because of the large difference in the heat capacity of the electrons and the phonons, they can be treated as two coupled subsystems. Before excitation, the electrons occupy the energy states below the Fermi level. Upon excitation of metallic thin films, or gold nanoparticles by ultrafast laser pulses, the energy is transferred to the electrons by absorption of photons via interband and intraband transition. The relaxation processes start to thermalize the electrons via electron-electron scattering and electron scattering with the surface. This thermalization process occurs in a few hundreds of femtoseconds [14]-[18]. The second step in the relaxation process is the transfer of the energy to the lattice via electron-phonon interaction. The last step in the relaxation is the energy transfer to the surrounding medium. The electron–electron and electron-phonon coupling processes and their dependence on the particle size were studied extensively [19]-[28], but how it affects the particle shape are not completely understood which is a target in this work.

Although there are several studies investigating the thermal stability of the gold nanoparticles in a solution, they are scattered and do not include the effect of all the shapes and surface coatings [29]-[33]. Some examples are: El-Sayed's group studied thermal stability of electrochemically prepared gold nanorods encapsulated inside the mixture of cetyltrimethylammonium bromide (CTAB) and tetraoctylammonium bromide (TDAB) rod shape micelles [21] and the mean aspect ratio of these nanorods in aqueous solution decreases with increasing the temperature. In another study, Petrova *et al*. [29] observed that gold nanorods at the highest temperature examined (250˚C) would transform into spheres within one hour. Al-Sherbini *et al.* [31] [32] studied the effect of the thermal heating and UV-light on gold nanorods with different aspect ratios in water/glycerol mixtures.

The objectives of this study are twofold that are continuation to our previous results [34]-[36]; 1) to investigate the role of shape and capping material on the thermal decomposition of gold nanoparticles as the stability enhancement is of interest for practical applications and 2) to investigate the dynamics of the hot carriers in the gold nanoparticles of different shapes, induced by femtosecond laser pulses.

2. Experimental Section

For the preparation of different shapes of gold nanoparticles, seeds and growth solutions were made as described below [34]-[36]:

Seeds solution: 2.5 ml of 0.2 M CTAB solution was mixed with 2.5 ml of 0.5 mM $HAuCl_4$. To the stirred solution, 30 µl of ice-cold 0.1M $NaBH_4$ was added, which resulted in the formation of a brownish yellow solution. Vigorous stirring of the seeds solution was continued for 2 minutes.

Growth solution: Different amounts (0, 0.1 and 0.25 ml) of 4mM $AgNO_3$ solution were added to 2.5 ml of 0.2 M CTAB solution. Then, 2.5 ml of 1 mM $HAuCl_4$ was added and after gentle mixing of the solution, 35 µl of 0.1 M ascorbic acid was added. Ascorbic acid as a reducing agent changes the growth solution from dark yellow to colorless within 10 minutes.

Next, the seeds solution was added to the growth solution. The color of the solution gradually changed within 10 - 20 minutes. To study thermal stability of gold nanoparticles, the change in the absorption spectrum of the gold nanoparticles solution was determined at different temperatures ranging from 40˚C to 220˚C in water bath (Transonic 46 O/H, USA). After the addition of a few drops of glycerol, the sample was heated above 100˚C in an oil bath in order to determine the decomposition temperature of the most stable micelles capping the gold nanoparticles. The same step was repeated by mixing nanoparticles with a solution of PVP. Thermal stability of gold nanoparticles has been followed by measuring the changes in absorption spectra as a function of time using the Perkin-Elmer Lambda 40 spectrometer. The particles were characterized by Transmission Electron Microscopy (TEM) with a Philips CM20 microscope, operating at an accelerating voltage of 200 KV.

Femtosecond Time-Resolved Transient Absorption Technique

The amplified Ti:sapphire laser system (spectraphysics) consists of two main components: One part is a pas-

sively mode-locked Ti:sapphire oscillator which is pumped by a diode-pumped, frequency-doubled Nd:Vandate laser (Coherent Verdi). The oscillator produces femtosecond laser pulses with pulse energies in the range of nJ. The output wavelength of the oscillator is set to 800 nm. The second main component is a regenerative amplifier which is pumped by a diode-pumped, frequency-doubled Nd:Vandate laser (Coherent Verdi) at repetition rate of 1 kHz. Since ultrashort laser pulses have high peak powers and can destroy the lasing medium the pulses generated in the oscillator part have to be stretched first before they can be injected into the amplifier. This is done by chirping the pulse using a grating. Later, after amplification another grating arranged in the opposite way compresses the pulse again to its original duration in the pulse compressor. This technique of amplifying the pulse energy is called chirped pulse amplification (CPA). The timing of the pulse injection (seeding) into the amplifier and ejection of the amplified pulse into the pulse compressor is controlled by a Pockels cell. The final outputs of this laser system are laser pulses of about 100 fs duration (full width at half maximum (FWHM)), with energy of 0.9 mJ at 800 nm at a repetition rate of 1 kHz.

A schematic overview of the optics of the femtosecond transient absorption spectrometer is given in **Scheme 1**. The output pulse from the amplified Ti:apphire laser system is split into three parts. A small part (4%) generates a white light continuum in a 1 mm sapphire plate which was used as the probe light. The pump source can be 400 and 266 nm laser pulses by SHG and third harmonic generation (THG). The pump pulse is delayed with respect to the probe pulse with an optical delay. Moving the delay line forward will decrease the distance the pump pulse has to travel and causes the pulse to arrive earlier in time with respect to the probe pulse whose travel distance remains constant. The delay line is computer controlled and allows a time resolution of 21 fs. The energies of the pump and probe pulses are adjusted with neutral density filters.

The probe light splits into a signal and a reference beam and the signal beam is overlapped at the sample position. The signal and reference beams are then focused into fiber optic cables and coupled into a monochromator for single wavelength measurements or a spectrograph for spectral measurements. The reference beam is split off beforehand and is directed towards a separate fiber optics cable.

The samples consisting of mainly transparent solutions are placed in a rectangular stationary cell or in cylindrical cell that can be rotated with a speed of 1000 rpm in order to ensure that a different part of the solution is exposed with each laser shot. Alternatively the solutions can be flowed through a rectangular cell by a micropump at a speed of roughly 125 μl/s. Experiments are performed at room temperature. All cells have an optical path length of 2 mm as the overlap of the probe and pump beam can only be achieved over this distance.

For recording single wavelength kinetic traces, the excitation beam is modulated by an optical chopper (HMS 221) with half the laser frequency (500 Hz). Hence only every other probe pulse monitors the changes in the sample induced by the pump pulse. This then causes an intensity modulation of the probe pulses, which varies with the same frequency of 500 Hz. A lock-in-amplifier can then be used to detect and measure very small Ac signals down to a few nanovolts. Accurate measurements may even be made when the signal is obscured by noise sources thousands of times larger like fluctuations in the laser light intensity of pump and probe pulses. The lock-in-amplifier uses a technique known as phase-sensitive detection to single out the component of the

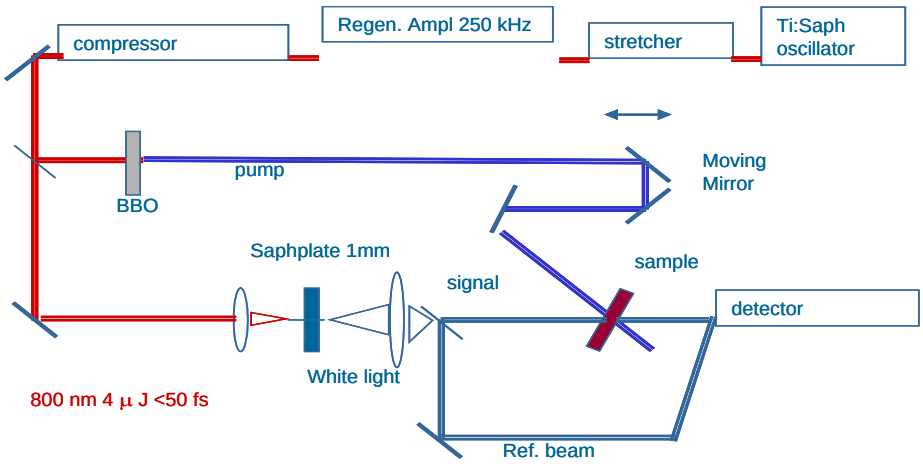

Scheme 1. Description of pump-probe transient setup.

signal at the specific reference frequency with which the pump pulse are modulated by the optical chopper. Noise signals at frequencies other than the reference frequency are then rejected and do not affect the measurement.

3. Results and Discussion

3.1. Shape and Morphology of Gold Nanoparticles

The seed method was successfully modified here in order to get more precise control in the shape of the gold nanoparticles. Anisotropic shapes of gold nanoparticles in **Figure 1** and **Figure 2** were formed by using different concentrations of silver ions and seeds solutions. The average size of the particles is determined from the transmission electron microscopic (TEM) and scanning tunneling microscope (STM) images and is found to be 5.0 ± 1.6 nm for the spheres, and rod length is 40.87 ± 6.1 nm, and its width 12.0 nm with aspect ratio a.r. = 3.4, and the prism is 41.12 ± 5.49 nm, and the thickness is about 9.1 nm (see **Figure 2**).

Our results indicate that the ratio of the Ag^+ concentration to the seed concentration is one of the key parameters for controlling the shape of the particles, e.g. spheres, rods, prisms or snapped prisms. Recently a new proposed mechanism for the formation of anisotropic gold nanoparticles was published that takes into account the reduction of Ag ions by ascorbic acid forming intermediate small Ag clusters, which can then act as a catalyst for the formation of gold nanoparticles by their adsorption onto the surface of the gold seeds [34] [36]-[38]. By controlling the concentration of silver ions that reduced to silver clusters and adjust the ratio with seeds concentration, gold spheres are formed as this ratio equal zero, rods as the ratio equal 1 and prisms are formed as the ratio equal 3 [34]. After controlling the shapes of gold nanostructures, the thermal stability of the formed particles was studied.

3.2. Thermal Stability of Gold Nanoparticles

The prepared gold nanoparticles are capped with only one surfactant (CTAB), and the anisotropic shape resulted by adding Ag^+ ions or clusters during particle growth [34]. It is important to understand the effect of surfactant structure on the stability of the formed micelles which represent the capping material of the gold particles. It is concluded that the Kraft temperature of the micelles depends on their chemical composition and the nature of the capping materials [28].

Figures 3(a)-(d) show the thermal stability of gold nanoparticles with different shapes. Gold nanospheres prepared in the absence of any Ag-ions or clusters, are not showing any change in the maximum absorption (**Figure 3(a)**) under thermal heating up to 180˚C. That is because the spherical shape of gold particles has the most stable facets {111} and these spheres capped with stable micelleses of CTAB.

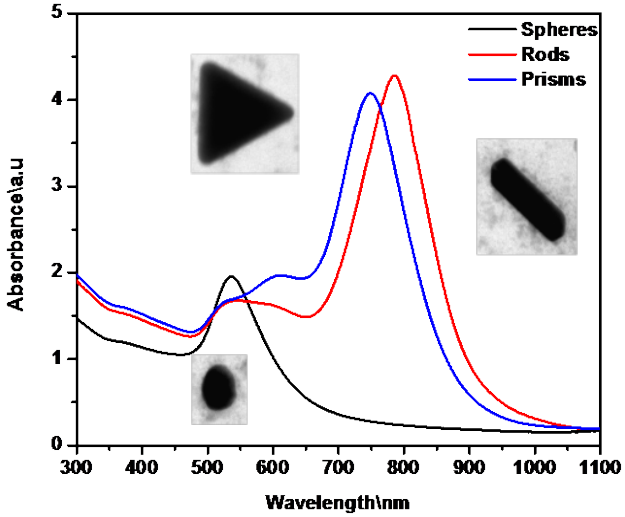

Figure 1. Absorption spectra show the formation of different shapes of gold nanoparticles using different volumes of $AgNO_3$ (0 ml for spheres, 0.1 ml for rods (a.r. = 3.4) and 0.25 for prisms).

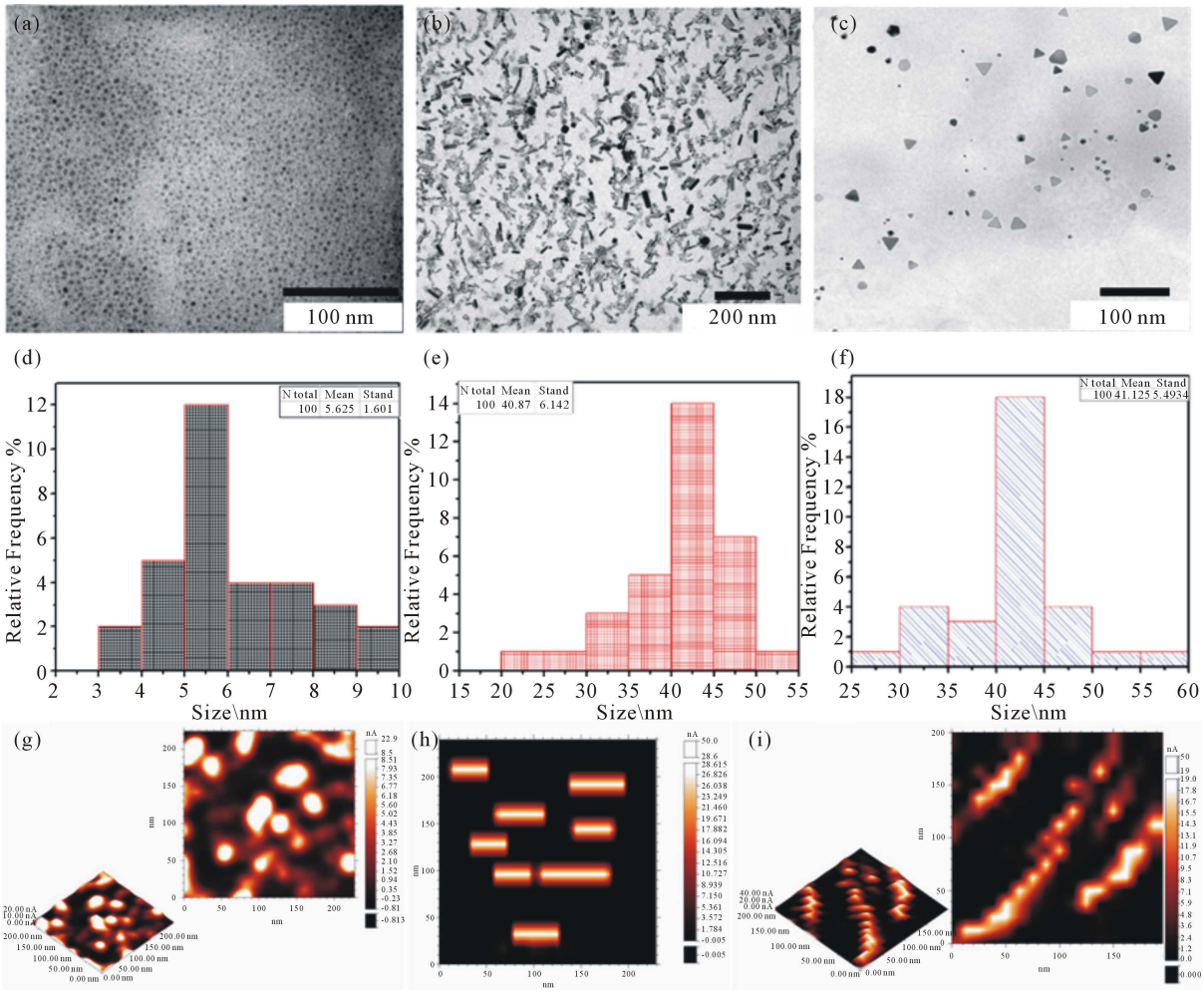

Figure 2. Shows TEM images of the formed gold nanostructures with different shapes: (a)-(c) spheres, rods and prisms respectively using different volumes of $AgNO_3$ (0 ml for spheres, 0.1 ml for rods (a.r. = 3.4) and 0.25 for prisms). The size distribution of the formed particles is shown below the TEM images (d)-(f) and STM images (g)-(i) respectively.

However, gold nanorods (**Figure 3(b)**) and nanoprisms (**Figure 3(c)**) here are decomposed under the thermal effect ranging from 40˚C to 180˚C. Since the gold particles are soluble in water which boil at 100˚C, few drops of glycerol has been added, and the sample was heated to 180˚C in an oil bath in order to determine the decomposition temperature of the most stable micelles capping the gold nanoparticles (**Figure 4**). Normalized absorption spectra (**Figure 3(d)**) show the difference in stability of the different shapes.

At each temperature, the change in the absorption spectrum was followed as a function of time. The rate of the change in the shape at each of these temperatures from that present at room temperature was determined by following the rate of the absorbance change of the absorption maximum of longitudinal plasmon band SP_L. From the values of the rate constants (first-order decay) at different temperatures, the activation energy (E_{act}) of the shape transformation can be calculated [28]. The activation energy for gold nanorods with aspect ratio 3.4 (7.41 ± 0.1 kJ·mol^{-1}) is lower than that for aspect ratio 2.2 (7.85 ± 0.2 kJ·mol^{-1}) and also lower than that of gold nanoprisms (7.94 ± 0.1 kJ·mol^{-1}) (see **Figure S1** and **Figure S2**).

Comparing these results with the data previously reported by El-Sayed and coworkers [5] [28] for the thermal stability of gold nanorods prepared with a mixture of two surfactants, it can be observed that the Kraft temperature of the rod shape micelles formed from CTAB (180˚C) is quite higher than that for the rod shape micelles which formed from a mixture of CTAB and TDAB as a co-surfactant (155˚C) because CTAB binds preferentially to the low-energy{111} and {110} crystallographic facets of the gold nanorods than the high-energy {100} crystallographic facets in case of CTAB and TDAB as a co-surfactant [39].

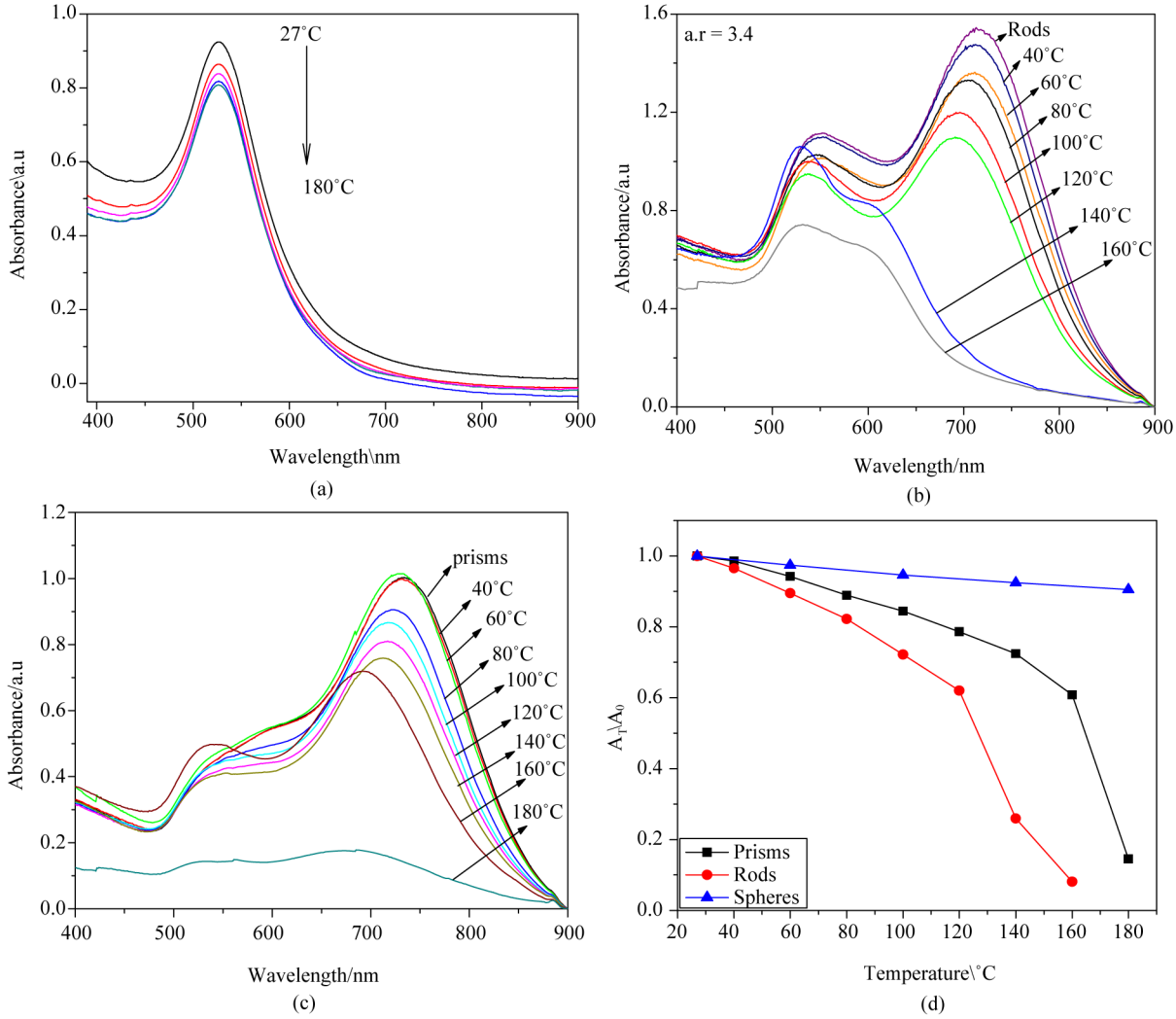

Figure 3. Absorption spectra show the thermal effect on gold nanospheres (a), gold rods of aspect ratio 3.4 (b) gold nanoprisms (c) and normalized absorption spectra of different shapes (d).

Temperature has different effects on gold nanoprisms than that observed here for the rods (see TEM images in **Figure 4**). For rods, the long rods are not stable, thus, they decompose leading to a decrease in the absorbance and blue shifted of the SP_L band. In case of nanoprisms, the third absorption band characterizing to the nanoprisms disappeared gradually giving absorption spectra similar to the rods. Absorbance and blue shift of the SP_L band took place and the effect of high temperature on nanoprisms can be summarized here in the following steps: 1) Dissolution of the tips of the prism shape which are unstable thermodynamically, giving snapped prisms. 2) These snapped prisms changed on their shape to reach the rod shape particles that are more stable thermodynamically. 3) The bigger particles decomposed leading to a decrease in the absorbance intensity and red shift to lower wavelength, but up to 160˚C, particles are still stable. Finally, the micelles are completely decomposed at 180˚C and the Kraft temperature has found to be ~185˚C (**Figure 3(c)**). The reason that gold nanoprisms are thermally stable than rods, is due to it has low-energy {111} crystallographic facets, however, gold rods have {110} crystallographic facets with {111} crystallographic facets [39]-[41].

3.3. Enhancement of Thermal Stability of Gold Nanoparticles

A solution of PVP is added as another stabilizer to the prepared gold nanoparticles capped with CTAB, and then their thermal stability was studied as mentioned above. Addition of 30% by weight of PVP to the nanorods solution leads to the complete stability of gold nanorods and effectively inhibits the deformation process. Upon

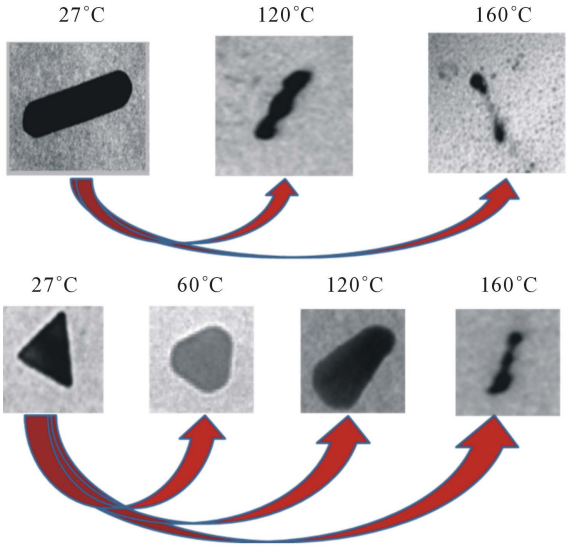

Figure 4. TEM-images showing the decomposition of gold nanorods (aspect ratio 3.4) and gold nanoprisms at different temperatures.

addition of PVP, a slight red shift (~4 nm) observed due to changing the dielectric constant of the surrounding medium and the absorbance decreased slightly as a result of decreasing the concentration of rods after addition of PVP. Afterwards, no more absorption shift was observed up to 220˚C (see **Figure 5(a)**). In case of nanoprisms, the particles are completely stable up to 100˚C after addition of 30% PVP, then slight decrease in the absorbance value observed with no shift in the absorption band up to 140˚C. At 160˚C, the intensity of their absorption band decreases remarkably, and the particles aggregated at 180˚C (see **Figure 5(b)**).

As the symmetry of the shape increases, as the stability decreases (**Figure 6**). One reason for the stability enhancement could be that the surfactant or polymer normally enhances the dispersivity of nanoparticles in the solution by modification of surface charges. By preventing the agglomeration between the gold nanoparticles, the thermal stability may increase under different temperature compared to the pristine gold nanomaterial. The preferential adsorption of PVP onto {110} faces of rods also plays an important role for the differentiation of distinct facets [42] [43]. Since the shape deformation of the gold nanorods and nanoprisms is affected by the Ostwald ripening, polymer like PVP coating on the nanorparticles as a second nanolayer could effectively increase the barrier of the dissolution or re-deposition processes in the Ostwald ripening, suppressing the shape deformation [33].

3.4. Hot Carrier Dynamics of Gold Nanoparticles of Different Shapes

The electron dynamics of different shapes gold nanoparticles (prisms, rods, and spheres in **Figure 1**) in solution are studied using a femtosecond pump probe setup which described in details in the experimental section. Single wavelength kinetics of the plasmon bleach recovery of gold nanoparticles of different shapes is recorded [11]. The pump wavelength was 400 nm in all experiments which were performed at room temperature. **Figure 7(a)** shows the difference in bleach intensity of different shapes of gold nanoparticles with different delay time. The decay curve of the gold nanorods after excitation with 400 nm laser pulse at different delay times and its fitting are shown in **Figure 7(b)**.

The power dependence of the relaxation dynamics of gold nanoparticles in hydrogel has been shown [41]. At low pump power, only a fast decay component of a few picoseconds is observed. By increasing the pump power, the fast component of the plasmon bleach recovery becomes longer and a second longer component (~100 ps) appears. The fast decay component is ascribed to the thermal equilibration between the hot electrons and the nanoparticle lattice by electron-phonon (e-ph) interactions while the slow decay component represents the further cooling of the gold nanoparticles by the heat conduction away from the hot lattice to the surrounding medium. The slow decay component has therefore been ascribed to phonon-phonon interactions (ph-ph), which

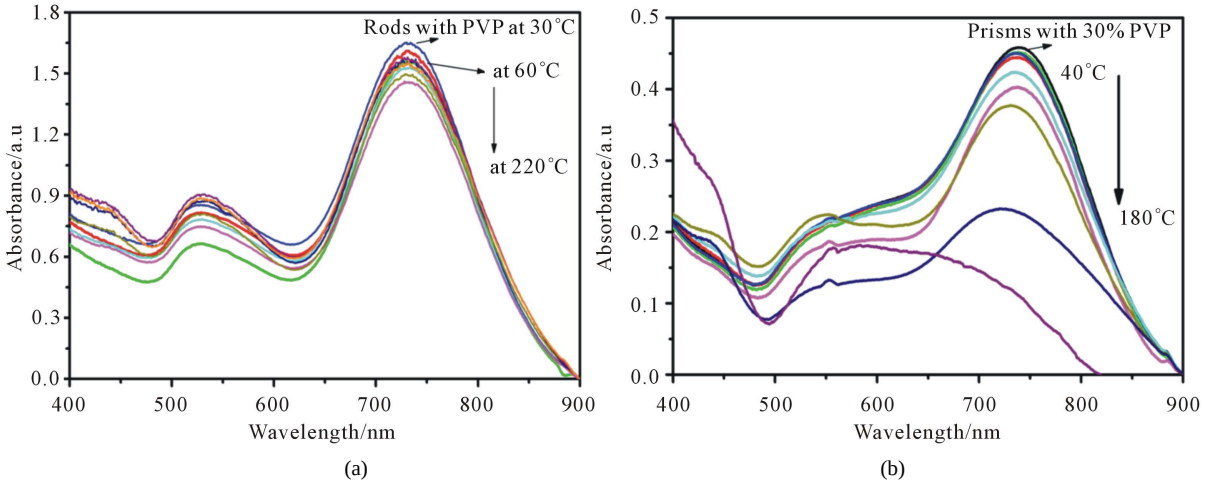

(a) (b)

Figure 5. Absorption spectra showing the effect of thermal heating on gold nanorods with 30% PVP from 40˚C to 220˚C. and (b) Absorption spectra showing the effect of the addition of 30% PVP on the thermal stability of the gold nanoprisms.

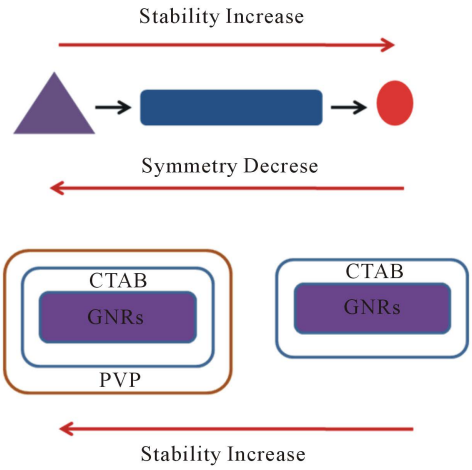

Figure 6. Schematic diagram shows the effect of shape symmetry and capping materials on the thermal stability.

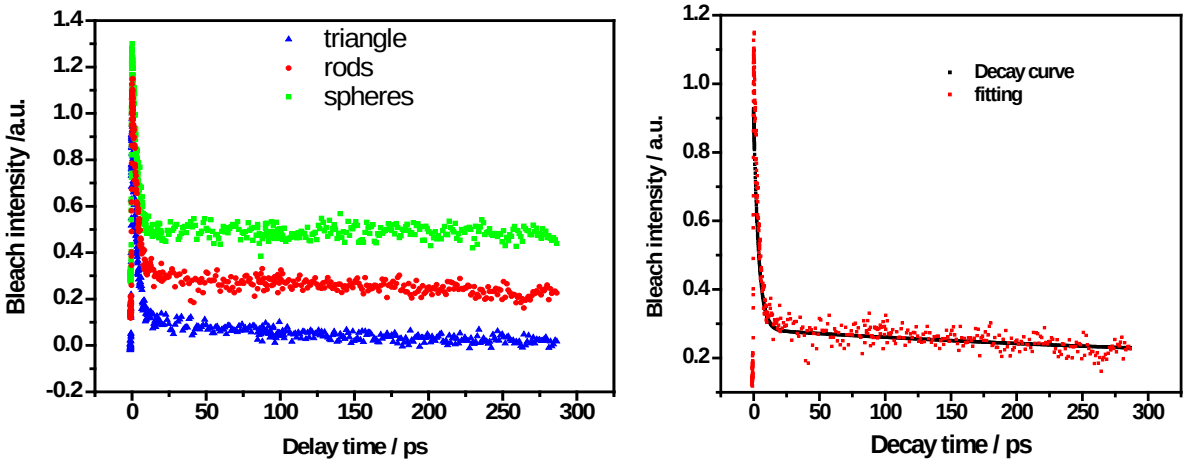

(a) (b)

Figure 7. Shows the difference in bleach intensity of different shapes of gold nanoparticles with different delay time (a) and (b) shows the fitting decay curve of the gold nanorods after excitation with 400 nm laser pulse at different delay times.

finally leads to the complete cooling of the nanoparticles. The reason for this power dependence of the electron-phonon relaxation time is that the heat capacity of the electron gas is temperature dependent [19] [21]. In addition, higher initial temperatures of the electron gas due to higher excitation powers with a more intense laser pulse will lead to a larger increase of the lattice temperature. If the subsequent removal of the heat by the surrounding medium is the rate-limiting step and depends on the temperature of the lattice, the appearance of second slow relaxation time can be qualitatively understood. More energy dumped into the nanoparticles will simply lead to longer relaxation times of the plasmon bleach because it takes longer for the whole system (gold nanoparticles and the host material) to cool down again.

While especially the electron-phonon coupling has been investigated in the low excitation regime before, it still remains a question, whether the slow phonon-phonon relaxation is mainly due to the heat exchange between the particle and the surrounding medium, or rather is limited by the conduction of the heat away from the particles within the surrounding matrix. Both processes would involve phonon-phonon interactions, but in the first case phonon-phonon coupling between the particles and the matrix is important while the latter would involve mainly the phonons of the surrounding matrix. Comparing the relaxation dynamics of gold nanoparticles of different shapes, it is clear that the relaxation time of the fast component is almost constant (~2.27 ps) in all the three samples. This means that the e-ph coupling has no dependence on the particle shape [8]. On the other hand, the slow component which refers to the ph-ph coupling is shape dependent. The ph-ph coupling is much slower in dots (~176 ps compared with spheres in reference 43 (~150 ps)) than in rods (~142 ps) and prisms (~115 ps) and this could be explained by the fact that nanoprisms have more surface area than that of the rods and the spheres. The Fermi-level also will be different because the presence of semiconducting silver clusters [44] [45] at the tips of rods and prisms that could do electron transfer with gold surface. As shown in our recently work, the concentration of Ag-clusters that used in the formation of prisms is higher than that used in rods, however gold spheres are formed in the absence of Ag-clusters. More studies are performed now to understand the effect of the presence of these clusters on the relaxation dynamics of nanoparticles.

4. Conclusion

We have shown here that the shape and capping materials play an important role in the thermal stability of gold nanostructures. The mechanism of particles dissociation in case of nanoprisms is different than that of nanorods under thermal heating. Great enhancement of the thermal stability has been achieved by adding specific amounts of PVP to the gold nanoparticles. The dynamics of the hot carriers in metallic nanodots, nanorods and nanoprisms induced by femtosecond laser pulses are investigated in gold nanoparticles. It is found that the ph-ph coupling is much slower in dots than in rods and prisms while e-ph coupling is almost the same in these particles. This is due to the large surface area of the nanoprisms compared with the rods or spheres of different thickness and electron transfer between the formed semiconducting Ag clusters and gold surface.

Acknowledgements

We acknowledge all the member of NILES-Cairo University specially professor Mona Bakr Mohamed for her support to us.

References

[1] Murphy, C.J., Sau, T.K., Gole, A.M., Orendorff, C.J., Gao, J., Gou, L., Hun Yadi, S.E. and Li, T. (2005) Anisotropic Metal Nanoparticles: Synthesis, Assembly, and Optical Applications. *The Journal of Physical Chemistry B*, **109**, 13857-13870. http://dx.doi.org/10.1021/jp0516846

[2] Shi, W., Zeng, H., Sahoo, Y., Ohulchansky, T.Y., Ding, Y., Wang, Z.L., Swihart, M. and Prasad, P.N. (2006) A General Approach to Binary and Ternary Hybrid Nanocrystals. *NANO Letters*, **6**, 875-881. http://dx.doi.org/10.1021/nl0600833

[3] Liang, H.-P., Wan, L.-J., Bai, C.-L. and Jiang, L.J. (2005) Gold Hollow Nanospheres: Tunable Surface Plasmon Resonance Controlled by Interior-Cavity Sizes. *The Journal of Physical Chemistry B*, **109**, 7795-7800. http://dx.doi.org/10.1021/jp045006f

[4] Jana, N.R., Gearheart, L. and Murphy, C.J. (2001) Evidence for Seed-Mediated Nucleation in the Chemical Reduction of Gold Salts to Gold Nanoparticles. *Chemistry of Materials*, **13**, 2313-2322. http://dx.doi.org/10.1021/cm000662n

[5] Nikoobakht, B. and El-Sayed, M.A. (2001) Evidence for Bilayer Assembly of Cationic Surfactants on the Surface of

Gold Nanorods. *Langmuir*, **17**, 6368-6374. http://dx.doi.org/10.1021/la010530o

[6] Nikoobakht, B. and El-Sayed, M.A. (2003) Preparation and Growth Mechanism of Gold Nanorods (NRs) Using Seed-Mediated Growth Method. *Chemistry of Materials*, **15**, 1957-1962. http://dx.doi.org/10.1021/cm020732l

[7] El-Sayed, M.A. (2001) Some Interesting Properties of Metals Confined in Time and Nanometer Space of Different Shapes. *Accounts of Chemical Research*, **34**, 257-264. http://dx.doi.org/10.1021/ar960016n

[8] Link, S. and El-Sayed, M.A. (2000) Shape and Size Dependence of Radiative, Non-Radiative and Photothermal Properties of Gold Nanocrystals. *International Reviews in Physical Chemistry*, **19**, 409-453. http://dx.doi.org/10.1080/01442350050034180

[9] Link, S. and El-Sayed, M.A. (2003) Optical Properties and Ultrafast Dynamics of Metallic Nanocrystals. *Annual Review of Physical Chemistry*, **54**, 331-366. http://dx.doi.org/10.1146/annurev.physchem.54.011002.103759

[10] Link, S., Burda C., Wang Z.L. and El-Sayed, M.A. (1999) Electron Dynamics in Gold and Gold-Silver Alloy Nanoparticles: The Influence of a Nonequilibrium Electron Distribution and the Size Dependence of the Electron-Phonon Relaxation. *The Journal of Chemical Physics*, **111**, 1255-1264. http://dx.doi.org/10.1063/1.479310

[11] Mohamed, M.B., Ahmadi, T.S., Link, S., Braun, M. and El-Sayed, M.A. (2001) Hot Electron and Phonon Dynamics of Gold Nanoparticles Embedded in a Gel Matrix. *Chemical Physics Letters*, **343**, 55-63. http://dx.doi.org/10.1016/S0009-2614(01)00653-4

[12] Link, S., Furube, A., Mohamed, M.B., Asahi, T., Masuhara, H. and El-Sayed, M.A. (2002) Hot Electron Relaxation Dynamics of Gold Nanoparticles Embedded in $MgSO_4$ Powder Compared to Solution: The Effect of the Surrounding Medium. *The Journal of Physical Chemistry B*, **106**, 945-955. http://dx.doi.org/10.1021/jp013311k

[13] Link, S., Hathcock, D.J., Nikoobakht, B. and El-Sayed, M.A. (2003) Medium Effect on the Electron Cooling Dynamics in Gold Nanorods and Truncated Tetrahedra. *Advanced Materials*, **15**, 393-396. http://dx.doi.org/10.1002/adma.200390088

[14] Cao, J.G., El-Sayed, A.H., Miller, R.J. and Mantell, D.A. (1998) Femtosecond Photoemission Study of Ultrafast Electron Dynamics in Single-Crystal Au(111) Films. *Physical Review B*, **58**, 10948-10952. http://dx.doi.org/10.1103/PhysRevB.58.10948

[15] Ogawa, S., Nagano, H. and Petek, H. (1998) Stability of a Photoinduced Insulator-Metal Transition in $Pr_{1-x}Ca_xMnO_3$. *Physical Review B*, **57**, Article ID: R15033. http://dx.doi.org/10.1103/PhysRevB.57.R15033

[16] Shahbazyan, T.V. and Perakis, I.E. (2000) Surface Collective Excitations in Ultrafast Pump-Probe Spectroscopy of Metal Nanoparticles. *Chemical Physics*, **251**, 37-49. http://dx.doi.org/10.1016/S0301-0104(99)00311-0

[17] Hodak, J.K., Martini, I. and Hartland, G.V. (1998) Spectroscopy and Dynamics of Nanometer-Sized Noble Metal Particles. *The Journal of Physical Chemistry B*, **102**, 6958-6967. http://dx.doi.org/10.1021/jp9809787

[18] Bigot, J.Y., Merle, J.C., Cregut, O. and Daunois, A. (1995) Electron Dynamics in Copper Metallic Nanoparticles Probed with Femtosecond Optical Pulses. *Physical Review Letters*, **75**, 4702-4705. http://dx.doi.org/10.1103/PhysRevLett.75.4702

[19] Shahbazyan, T.V., Perakis, I.E. and Bigot, J.Y. (1998) Size-Dependent Surface Plasmon Dynamics in Metal Nanoparticles. *Physical Review Letters*, **81**, 3120-3123. http://dx.doi.org/10.1103/PhysRevLett.81.3120

[20] Roberti, T.W., Smith, B.A. and Zhang, J.Z. (1995) Ultrafast Electron Dynamics at the Liquid-Metal Interface: Femtosecond Studies Using Surface Plasmons in Aqueous Silver Colloid. *The Journal of Chemical Physics*, **102**, 3860. http://dx.doi.org/10.1063/1.468545

[21] Faulhaber, A.E., Smith, B.A., Andersen, J.K. and Zhang, J.Z. (1996) Femtosecond Electronic Relaxation Dynamics in Metal Nano-Particles: Effects of Surface and Size Confinement. *Molecular Crystals and Liquid Crystals Science and Technology*, **283**, 25-30. http://dx.doi.org/10.1080/10587259608037859

[22] Smith, B.A., Zhang, J.Z., Giebel, U. and Schmid, G. (1997) Direct Probe of Size-Dependent Electronic Relaxation in Single-Sized Au and Nearly Monodisperse Pt Colloidal Nano-Particles. *Chemical Physics Letters*, **270**, 139-144. http://dx.doi.org/10.1016/S0009-2614(97)00339-4

[23] Del Fatti, N., Flytzanis, C. and Vallee, F. (1999) Ultrafast Induced Electron-Surface Scattering in a Confined Metallic System. *Applied Physics B*, **68**, 433-437. http://dx.doi.org/10.1007/s003400050645

[24] Hodak, J.K., Martini, I. and Hartland, G.V. (1998) Ultrafast Study of Electron-Phonon Coupling in Colloidal Gold Particles. *Chemical Physics Letters*, **284**, 135-141. http://dx.doi.org/10.1016/S0009-2614(97)01369-9

[25] Smith, B.A., Waters, D.M., Faulhaber, A.E., Kreger, M.A., Roberti, T.W. and Zhang, J.Z. (1997) Preparation and Ultrafast Optical Characterization of Metal and Semiconductor Colloidal Nano-Particles. *Journal of Sol-Gel Science and Technology*, **9**, 125-137.

[26] Hodak, J.K., Martini, I. and Hartland, G.V. (2000) Electron-Phonon Coupling Dynamics in Very Small (Between 2 and 8 nm Diameter) Au Nanoparticles. *The Journal of Chemical Physics*, **112**, 5942.

http://dx.doi.org/10.1063/1.481167

[27] Sun, Y. and Xia, Y.J. (2004) Mechanistic Study on the Replacement Reaction between Silver Nanostructures and Chloroauric Acid in Aqueous Medium. *Journal of the American Chemical Society*, **126**, 3892-3901. http://dx.doi.org/10.1021/ja039734c

[28] Mohamed, B.M., Ismail, K.Z., Link, S. and El-Sayed, M.A. (1998) Thermal Reshaping of Gold Nanorods in Micelles. *The Journal of Physical Chemistry B*, **102**, 9370-9374. http://dx.doi.org/10.1021/jp9831482

[29] Petrova, H., Perez Juste, J., Pastoriza-Santos, I., Hartland, G.V., Liz-Marzan, L.M. and Mulvaney, P. (2006) On the Temperature Stability of Gold Nanorods: Comparison between Thermal and Ultrafast Laser-Induced Heating. *Physical Chemistry Chemical Physics*, **8**, 814-821. http://dx.doi.org/10.1039/B514644E

[30] Veith, G.M., Lupini, A.R., Rashkeev, S., Pennycook, S.J., Mullins, D.R., Schwartz, V., Bridges, C.A. and Dudney, N.J. (2009) Thermal Stability and Catalytic Activity of Gold Nanoparticles Supported on Silica. *Journal of Catalysis*, **262**, 92-101. http://dx.doi.org/10.1016/j.jcat.2008.12.005

[31] Al-Sherbini, M.E. (2010) UV-Visible Light Reshaping of Gold Nanorods. *Materials Chemistry and Physics*, **121**, 349-353. http://dx.doi.org/10.1016/j.matchemphys.2010.01.048

[32] Al-Sherbini, M.E. (2004) Thermal Instability of Gold Nanorods in Micellar Solution of Water/Glycerol Mixtures. *Colloids and Surfaces A*: *Physicochemical and Engineering Aspects*, **246**, 61-69. http://dx.doi.org/10.1016/j.colsurfa.2004.06.038

[33] Zou, R.X., Zhang, Q., Zhao, Q., Peng, F., Wang, H.J., Yu, H. and Yang, J. (2010) Thermal Stability of Gold Nanorods in an Aqueous Solution. *Colloids and Surfaces A*: *Physicochemical and Engineering Aspects*, **372**, 177-181. http://dx.doi.org/10.1016/j.colsurfa.2010.10.012

[34] Attia, Y., Buceta, D., Blanco-Varela, C., Mohamed, M., Barone, G. and López-Quintela, M.A. (2014) Structure-Directing and High-Efficiency Photocatalytic Hydrogen Production by Ag Clusters. *Journal of the American Chemical Society*, **136**, 1182-1185.

[35] Attia, Y., Flores-Arias, M., Nieto, D., Vázquez-Vázquez, C., De La Fuente, G. and López-Quintela, M. (2015) Transformation of Gold Nanorods in Liquid Media Induced by nIR, Visible, and UV Laser Irradiation. *The Journal of Physical Chemistry C*, **119**, 13343-13349.

[36] Attia, Y., Buceta, D., Requejo, F., Giovanetti, L. and López-Quintela, M. (2015) Photostability of Gold Nanoparticles with Different Shapes: The Role of Ag Clusters. *Nanoscale*, **7**, 11273-11279. http://dx.doi.org/10.1039/C5NR01887K

[37] Ledo-Suárez, A., Rivas, J., Rodríguez-Abreu, C.F., Rodríguez, M.J., Pastor, E., Hernández-Creus, A., Oseroff, S.B. and López-Quintela, M.A. (2007) Facile Synthesis of Stable Subnanosized Silver Clusters in Microemulsions. *Angewandte Chemie International Edition*, **46**, 8823-8827. http://dx.doi.org/10.1002/anie.200702427

[38] Rodríguez-Vázquez, M.J., Blanco, M.C., Lourido, R., Vázquez-Vázquez, C., Pastor, E., Planes, G.A., Rivas, J. and López-Quíntela, M.A. (2008) Synthesis of Atomic Gold Clusters with Strong Electrocatalytic Activities. *Langmuir*, **24**, 12690-12694. http://dx.doi.org/10.1021/la8018474

[39] Wang, Z.L., Mohamed, M.B., Link, S. and El-Sayed, M.A. (1999) Crystallographic Facets and Shapes of Gold Nanorods of Different Aspect Ratios. *Surface Science*, **440**, L809-L814. http://dx.doi.org/10.1016/S0039-6028(99)00865-1

[40] Marzbanrad, E., Rivers, G., Peng, P., Zhaoac, B. and Zhou, N.Y. (2015) How Morphology and Surface Crystal Texture Affect Thermal Stability of a Metallic Nanoparticle: The Case of Silver Nanobelts and Pentagonal Silver Nanowires. *Physical Chemistry Chemical Physics*, **17**, 315-324. http://dx.doi.org/10.1039/C4CP04129A

[41] Wang, Z.L. (2000) Transmission Electron Microscopy of Shape-Controlled Nanocrystals and Their Assemblies. *The Journal of Physical Chemistry B*, **104**, 1153-1175. http://dx.doi.org/10.1021/jp993593c

[42] Chen, J., Wiley, B.J. and Xia, Y. (2007) One-Dimensional Nanostructures of Metals: Large-Scale Synthesis and Some Potential Applications. *Langmuir*, **23**, 4120-4129. http://dx.doi.org/10.1021/la063193y

[43] Sun, Y., Mayers, B., Herricks, T. and Xia, Y. (2003) Polyol Synthesis of Uniform Silver Nanowires: A Plausible Growth Mechanism and the Supporting Evidence. *Nano Letters*, **3**, 955-960. http://dx.doi.org/10.1021/nl034312m

[44] Chen, W. and Chen, S. (2014) RSC Smart Materials No. 7. RSC, Cambridge.

[45] Piñeiro, Y., Rivas, J. and López-Quintela, M.A. (2014) The Emergence of Quantum Confinement in Atomic Quantum Clusters. In: Berti, D. and Palazzo, G., Eds., *Colloidal Foundations of Nanoscience*, Elsevier, Amsterdam, 81-105.

Supplementary Information

Thermal stability of gold nanorods with different aspect ratios (2.2 and 4.5):

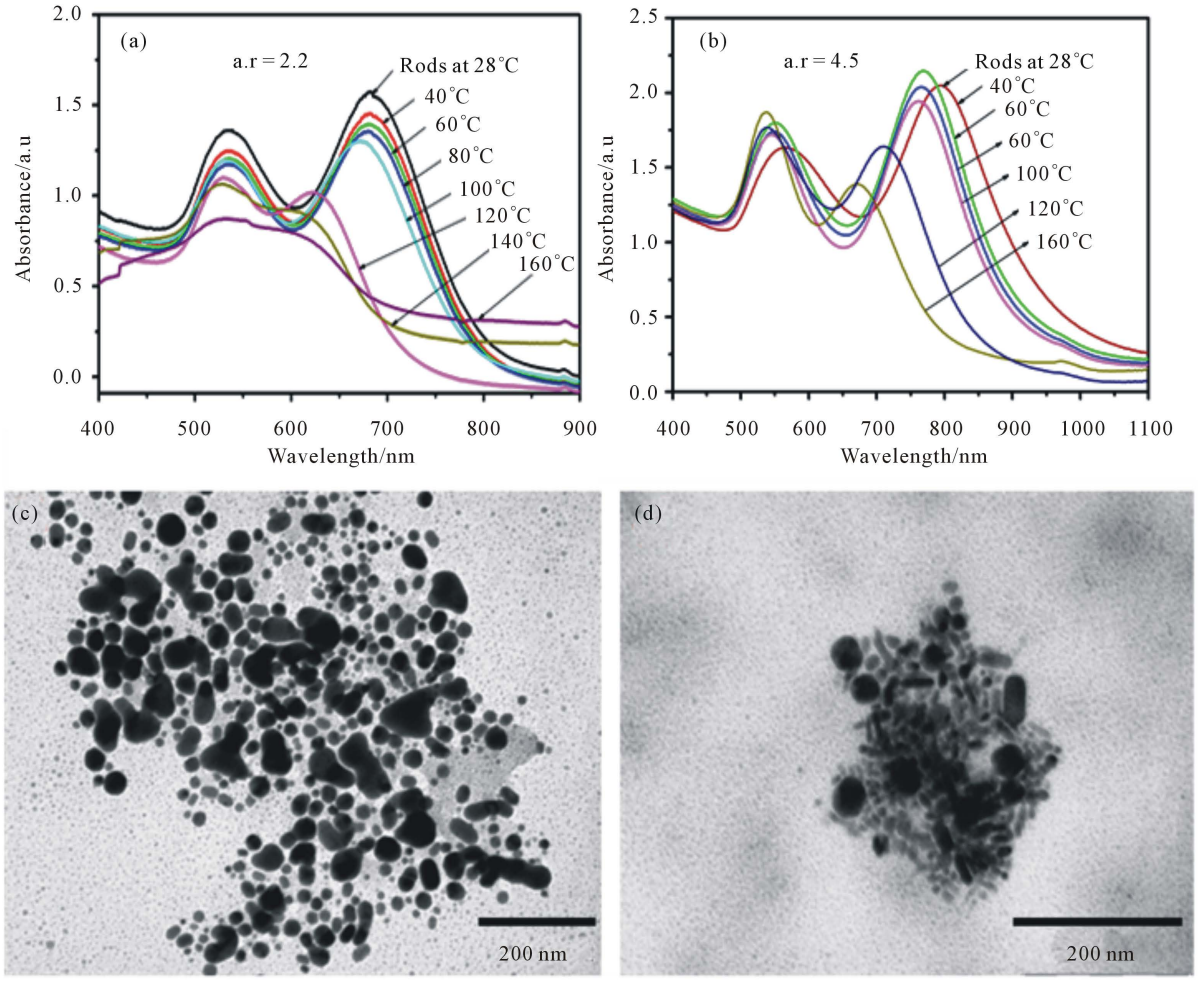

Figure S1. Absorption spectra showing the thermal effect on gold rods of aspect ratio 2.2 (a), and 4.5 (b). TEM-images for gold nanorods (c) with aspect ratio 3.4 at 160˚C and gold nanorods (d) with aspect ratio 4.5 at 160˚C.

Activation energies of different aspect ratios of gold nanorods and in the presence of PVP:

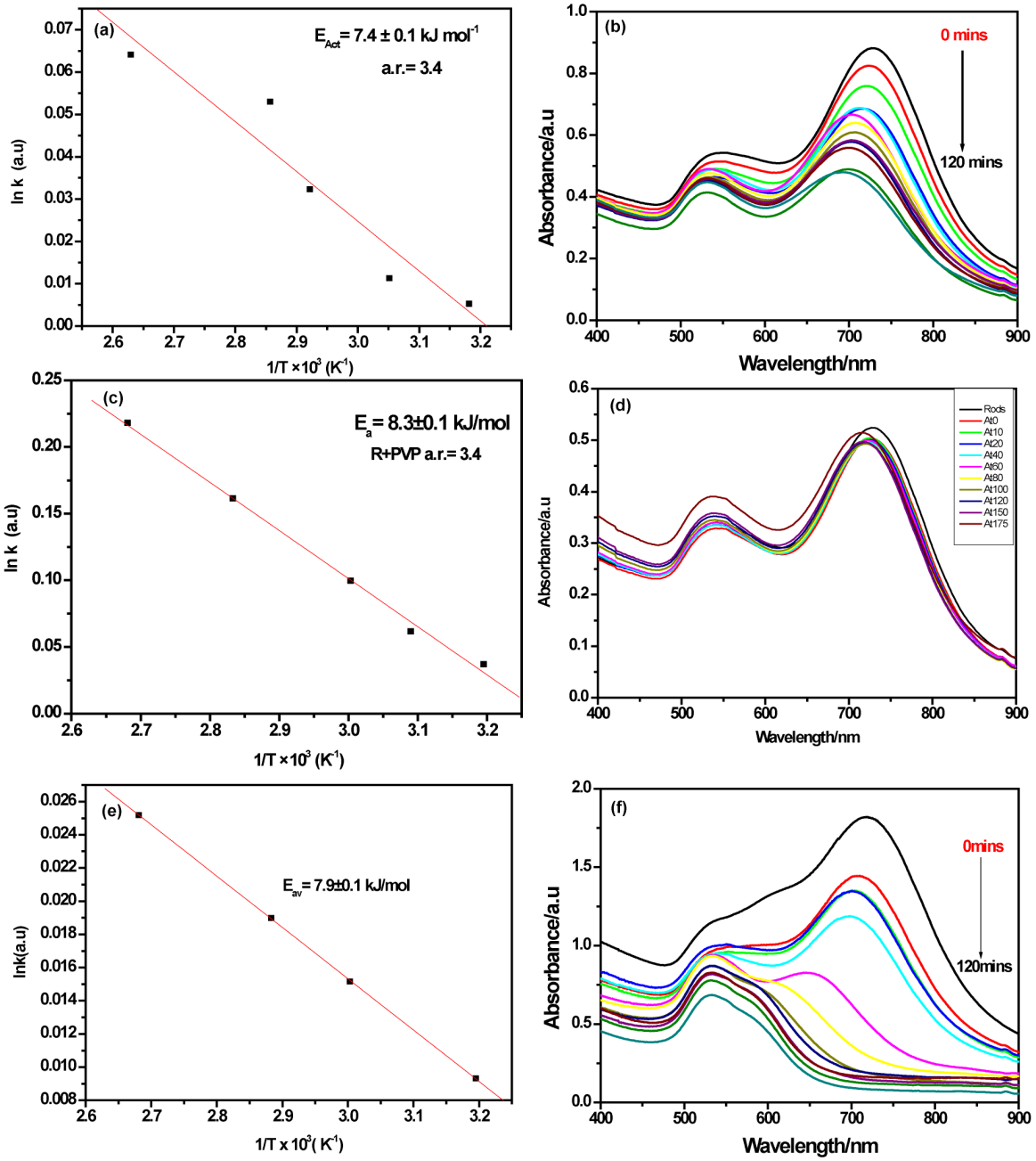

Figure S2. (a) & (b) The activation energies for gold nanorods with aspect ratio 3.4 and absorption spectra of that gold nanorods at 100˚C as a function of time, (c) & (d) for gold nanorods with aspect ratio 3.4 with PVP and (e) & (f) for gold nanoprisms are shown respectively.